

NUMERICAL SIMULATION OF A MICROCHANNEL FOR MICROELECTRONIC COOLING

WONG WAI HING¹ & NORMAH MOHD. GHAZALI²

Abstract. The paper discusses the numerical simulation of a micro-channel heat sink in microelectronics cooling. A three-dimensional Computational Fluid Dynamics (CFD) model was built using the commercial package, FLUENT, to investigate the conjugate fluid flow and heat transfer phenomena in a silicon-based rectangular microchannel heatsink. The model was validated with past experimental and numerical work for Reynolds numbers less than 400 based on a hydraulic diameter of 86 μ m. The investigation was conducted with consideration of temperature-dependent viscosity and developing flow, both hydrodynamically and thermally. The model provided detailed temperature and heat flux distributions in the microchannel heatsink. The results indicate a large temperature gradient in the solid region near the heat source. The highest heat flux is found at the side walls of the microchannel, followed by top wall and bottom wall due to the wall interaction effects. Silicon is proven to be a better microchannel heatsink material compared to copper and aluminum, indicated by a higher average heat transfer. A higher aspect ratio in a rectangular microchannel gives higher cooling capability due to high velocity gradient around the channel when channel width decreases. Optimum aspect ratio obtained is in the range of 3.7 - 4.1.

Keywords: Microchannel, CFD, FLUENT, numerical simulation, microelectronics cooling

Abstrak. Kertas kerja ini membincangkan simulasi berangka ke atas sinki haba saluran mikro dalam penyejukan alatan mikroelektronik. Model Dinamik Bendalir Berkomputer (CFD) tiga dimensi dibina menggunakan pakej komersil, FLUENT, untuk mengkaji fenomenon aliran bendalir dan pemindahan haba konjugat di dalam suatu sinki haba segi empat yang diperbuat daripada silikon. Model ditentusahkan dengan keputusan daripada uji kaji dan pengkajian berangka yang lepas untuk lingkungan nombor Reynolds kurang daripada 400 berdasarkan diameter hidraulik 86 μ m. Kajian ini mengambil kira kesan kelikatan bendalir yang bersandaran dengan suhu dan keadaan aliran pra-membangun dari segi hidrodinamik dan haba. Model memberi maklumat tentang taburan suhu dan fluks haba yang terperinci di dalam sinki haba saluran mikro. Kecerunan suhu yang tinggi dicatat pada kawasan pepejal berdekatan dengan sumber. Fluks haba paling tinggi didapati pada dinding tepi saluran mikro diikuti oleh dinding atas dan bawah. Purata pekali pemindahan haba yang lebih tinggi bagi silikon menjadikan ia bahan binaan sinki haba saluran mikro yang lebih baik berbanding dengan kuprum dan aluminium. Peningkatan nisbah aspek saluran mikro yang bersegi empat memberi kecekapan penyejukan yang lebih tinggi kerana kelebaran saluran yang berkurangan memberi kecerunan halaju yang lebih tinggi dalam saluran. Nisbah aspek yang optimum yang diperolehi adalah dalam lingkungan 3.7 - 4.1.

Kata kunci: Saluran mikro, CFD, FLUENT, simulasi berangka, penyejukan mikroelektron

¹ Email: waihing.wong@gmail.com

² Faculty of Mechanical Engineering, Universiti Teknologi Malaysia, 81310 Skudai, Johor, Malaysia
Email: normah@fkm.utm.my

1.0 INTRODUCTION

The industry of microelectronics has undergone rapid advancement in the past two decades. The high performance demand in the technology leads to large circuit integration for multifunction purposes. The technology trend goes in two directions, namely miniaturization in size and increase of power usage. This adds up the thermal challenges to microelectronics design. Referring to the international technology roadmap for semiconductors published in year 2002, the highest power density found in high-end workstation with 0.022 μm technology has a heat density approaching 100 W/cm^2 [1]. This high heat density is actually of the same order of magnitude as heat flux densities in nuclear reactors. Hence, thermal management in microelectronics design is vital.

For thermal management, various types of cooling methods for microelectronics devices have been developed. Examples include extended surface (fins) with turbulators, the highly parallel air and liquid impingement systems, modular internal conduction enhancement, and indirect and direct liquid cooling with water and dielectric coolants. The implementation of manifold microchannel heatsink, cooling micro heat pipes, pool boiling, multi-phase flow, liquid metal heatsink and microchannel heatsink are also proposed for the cooling solution in microelectronics.

Generally, microchannel cooling method is compact with high heat transfer rate due to a large surface area to volume ratio. Researches showed that the heat transfer coefficient is inversely proportional to the channel hydraulic diameter. Microchannels having a dimension of sub-millimeter scale surely provides comparatively high heat transfer rate than that in a conventional-sized channel.

Microchannels are advantageous due to its possibility in Multi-chip Module (MCM) integration. Integrated Circuit (IC) fabrication techniques used in constructing a microchannel heatsink make the MCM integration possible. As a result, microchannels cooling method provides a fully integrated, efficient, rugged, and compact design. Implementation of cooling technology using microchannels can remarkably reduce the contact thermal resistance in the cooling section which is considered as the main cause of cooling rate increase.

Some drawbacks in microchannel cooling include the high heat flux dissipation which leads to large pressure gradients. Therefore, advanced micro-pumping technologies are required to create the steady force convection in micro-channels. The implementation of this technology is still in its infancy. Major obstacles in implementing this technology are due to the lack of substantial understanding in the behavior of microchannel system. There are many challenges in microchannel fluid mechanics and heat transfer study. Therefore, scientific approach in analyzing the fluid flow and heat transfer behavior in microchannel is essential in developing a viable cooling solution.

Microchannel investigations have been done by many researchers in Europe and Japan. A study on a rectangular microchannel heatsink by Peng *et al.* [2] found that

cross-sectional aspect ratio had significant influence on the flow friction and convective heat transfer in both laminar and turbulent flows. Kawano *et al.* [3] provided experimental data on the friction and heat transfer in rectangular, silicon based microchannel heats sinks. It was found that the heat transfer efficiency of the heat exchanger indicated by thermal resistance is in the range of $0.1 \text{ Kcm}^2/\text{W}$ and the pressure loss can be predicted from the theoretical values of the fully developed flow inside the channel to the level of $Re = 200$. A number of numerical studies [4-7] were conducted based on the experimental work of Kawano. The simulations were completed through the conventional Navier-Stokes continuum model using different approaches like employment of self-developed SIMPLE (Semi-Implicit Method for Pressure Linked equation) algorithm [5] and Tri-Diagonal Matrix Algorithm (TDMA) [6]. The thermophysical properties of the cooling fluid were taken as either constant [5] or temperature dependent [4], and the flow was either fully developed [5] or developing [4]. Different degrees of agreement with the experimental results were found. The deviations observed in the recent studies are decreasing. A possible explanation of this trend is due to the dramatic improvement of the techniques of micro-fabrication resulting in little surface roughness in the channel walls. Another possible explanation is related to the recent experimental data having an increased reliability and accuracy [7].

Numerical investigations can provide a good alternative to study the complicated fluid flow and heat transfer phenomenon in microchannels. From previous studies, continuum model provided a good approach for the study purpose. Thus, FLUENT, a commercial package which also employs continuum model of Navier Stokes with SIMPLE algorithm is used for this investigation. The software is easily available, and most research and development departments in the industries and higher institutions have it. The numerical solver codes are well-established and thus provide a good start to more complex heat transfer and fluid flow problems that may require specialized codes for very specific problems. FLUENT provides adaptability to variation of material thermophysical properties with respect to temperature effect.

2.0 PROBLEM IDENTIFICATION

The physical model referred to is the heat exchanger prototype developed by Kawano *et al.* [3] as shown in Figure 1. It shows the outline of the microchannel heat exchanger embedded in a semiconductor device. Two silicon substrates, comprising a channel plate with deep grooves and a cover plate with an etched rectangular coolant inlet and outlet (for sumps) are bonded to form channels. The coolant is supplied via one of the two sumps and discharged from the other sump.

The physical model was focused on the fluid flowing inside a microchannel cavity of the microchannel heat collector. Heat transport in the unit cell is a conjugate problem which combines heat conduction in the solid and convective heat transfer

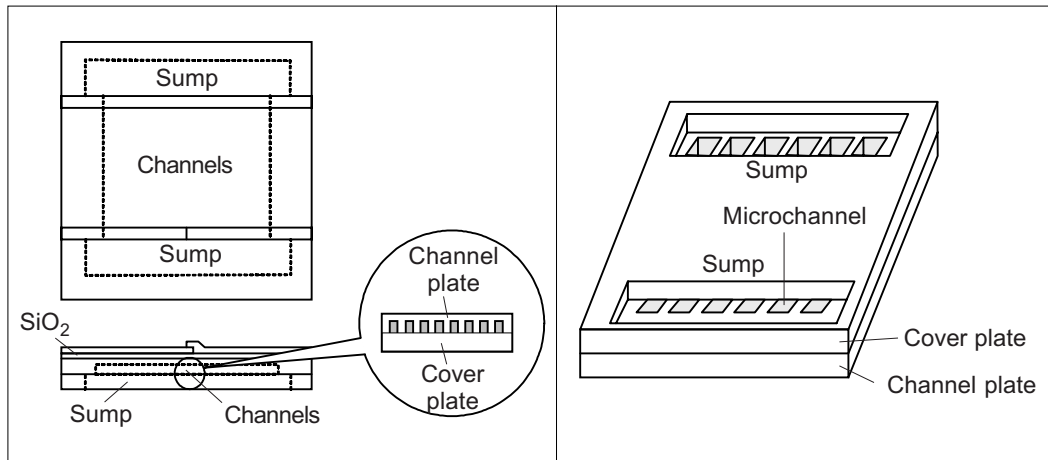


Figure 1 Semiconductor silicon chip embedded with microchannel heat exchanger

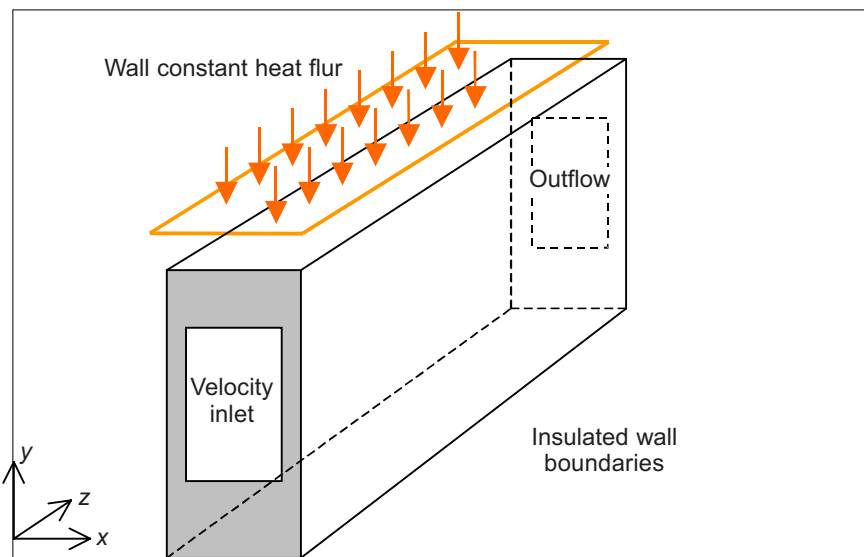


Figure 2 A unit cell of a microchannel as the modeling domain and its boundary conditions

to the coolant (water). A unit cell is shown in Figure 2 with the cross section and associated geometrical dimensions shown in Figure 3 and Table 1 respectively.

The two heat transfer modes are coupled by the continuities of temperature and heat flux at the interface between the solid and the fluid. The domain of analysis is constrained to the fluid flowing inside the microchannel heatsink. Hence, the analysis domain starts and ends within the fluid region entering and leaving the heatsink microchannel cavity. The fluid flow entering each cavity in the microchannel heatsink

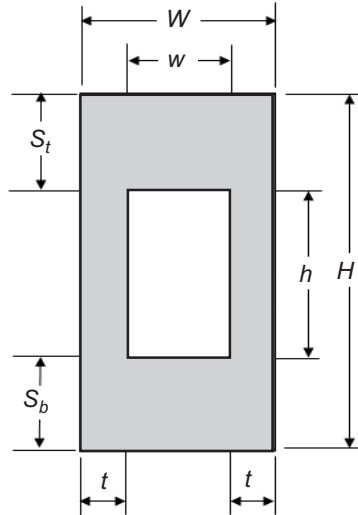


Figure 3 A cross-section of a microchannel unit cell

Table 1 Geometrical dimensions (MM) of a microchannel unit cell

H	900
W	100
h	180
w	57
S_t	450
S_b	270
t	21.5

is considered uniform. It is sufficient to take a unit cell consisting of only one channel and the surrounding solid as the computational domain. The results obtained can then be extended to the entire heatsink.

The critical fluid flow parameter in this investigation is pressure loss. This parameter is paramount to determine the friction loss in the heat exchanger and hence specify the pumping power for heat exchanger. Meanwhile, heat transfer efficiency of the heat exchanger is evaluated by the parameter of thermal resistance at inlet and outlet of the heat exchanger. Thermal stress is a critical issue in semiconductor designing. Therefore, investigation of the temperature distribution in the microstructure is important.

According to Kakac *et al.* [8], constant heat flux is applied when the heat source comes from electric resistance heating. Therefore, the cell unit of a microchannel is

assumed to have a constant heat flux, q'' at the top wall. In this investigation, the model used for validation to experimental data has a heat flux value of 90 W/cm^2 or $9 \times 10^5 \text{ W/m}^2$. The other wall boundaries of the solid region are assumed perfectly insulated with zero heat flux. The water flow velocities are taken from different Reynolds numbers, from 86 to 364, with reference to the hydraulic diameter of 86 mm, calculated based on:

$$u_m = \frac{\mu \cdot \text{Re}}{\rho \cdot D_h} \quad (1)$$

At the channel inlet, the water temperature is equal to a given constant inlet temperature of $T_{in} = 293 \text{ K}$. The outflow condition is assumed where there is no gradient in temperature, velocity and pressure. Some simplified assumptions are required to apply the modeling conditions to the heat transfer process in the heatsink. The major assumptions are:

- (i) Steady state flow and heat transfer.
- (ii) Laminar flow.
- (iii) Uniform wall heat flux.
- (iv) Uniform inlet velocity.
- (v) Negligible radiation heat transfer.

3.0 MODEL VALIDATION

Model validation of the results of present study is done in two stages: grid independence test and results validation with previous experimental and numerical study works.

3.1 Grid Independence Test

The model is tested for grid-independence to give proper resolution to the region where large gradients of fluid flow and heat transfer characteristic is predicted. The optimum grid system has the meshing resolution as shown in Figures 4 and 5.

Resolution to the development of fluid and thermal region is accommodated. A compressed non-uniform grid near the wall boundaries is adopted to properly resolve the viscous shear layer of the fluid flow. Besides, the meshing is also concentrated along the axial direction at the entrance of the channel to resolve the developing length. The meshing along the axial direction away from the entrance region has a relatively coarse grid system due to the insignificant change of fluid flow and heat transfer in transverse direction of the flow.

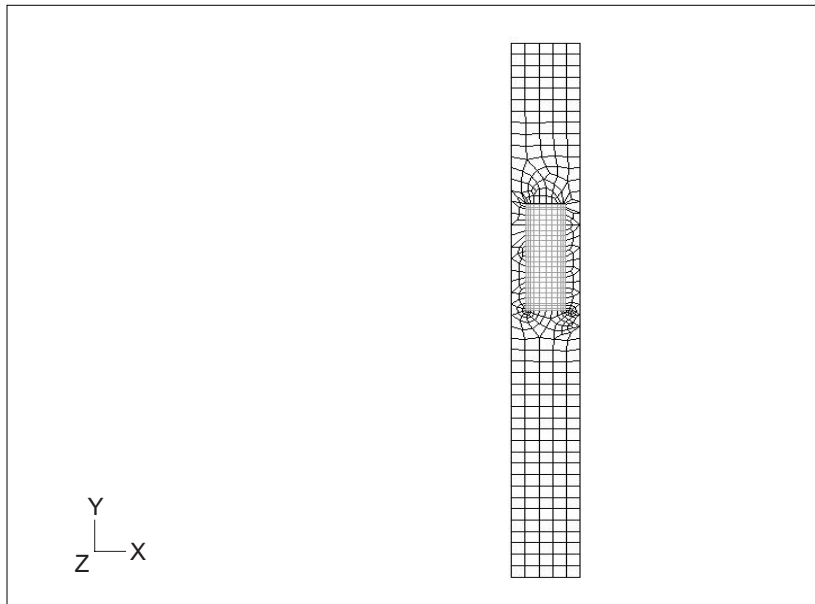


Figure 4 Pavé meshing of the rectangular hollow solid channel surrounding the fluid region in cut section view

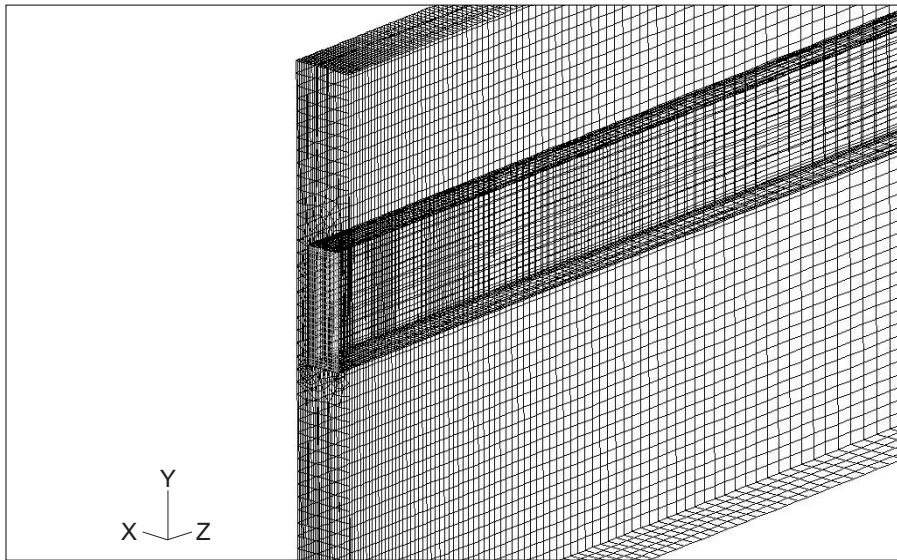


Figure 5 Optimum grid system of complete model

3.2 Model Validation with Previous Experimental and Numerical Studies

The model of the present study is validated using two parameters: thermal resistance and Poiseuille constant,

$$R_{t,out} = \frac{T_{w,out} - T_{in}}{q''} \quad (2)$$

$$C = f \cdot Re \quad (3)$$

where

$$f = \frac{2D_h(P_{in} - P_{out})}{\rho u_m L} \quad (3a)$$

$$Re = \frac{\rho u_m D_h}{\mu} \quad (3b)$$

Figure 6 shows model validation using Poiseuille constants. It is found that the numerical results are comparable to the experimental results. The predicted results in this study lie within the range of the experimental uncertainties, which are outlined by error bars. Poiseuille constant measured in this model demonstrates a linear proportion in relation with the Reynolds number. The results of the model are likely to have an under-prediction trend compared to the experimental results baseline.

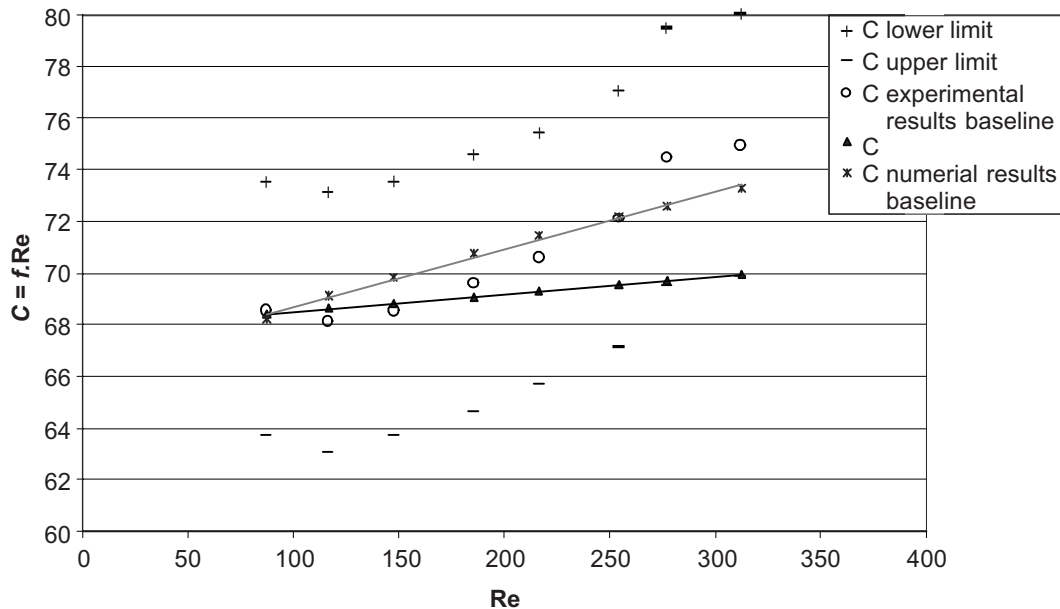


Figure 6 Model validation using Poiseuille constant

This phenomenon is due to the increasing developing length for higher Reynolds numbers. Compared to previous numerical work [2], present study yields a slightly under prediction of the Poiseuille constants at higher Reynolds numbers. Improvement of the Poiseuille constants measurements given by the numerical model in present study can be achieved by following Fedorov’s approach to include the effects of dependency on temperature for other thermophysical properties, such as density and specific heat, C_p . However, for an investigation of thermal efficiency of microchannel heatsink, this modification of the model is not recommended since it will increase dramatically the computation time and yet the variation from the results given by the original model is predicted not significant, as indicated by the trend in Figure 8.

Figure 7 shows the model validation using thermal resistance at the outlet region. The results yield good agreement with the experimental results for all Reynolds numbers. They lie within the acceptance of experimental results, outlined by the error bars. It is significant that the present model demonstrates a better agreement with the experimental results in the thermal resistance predictions compared to the model developed in Fedorov’s numerical work. The significant improvement of accuracy results given by the model in the present study is possibly due to the increase of density of grid system. Fedorov only employed a grid system with a unit grid dimension of $10 \times 20 \times 60$ in x, y and z -direction respectively. The model in this study uses a unit grid dimension of $8 \times 8 \times 50$. This improves the resolution of the results significantly and yields a better agreement to the experimental results. The average deviation for the present study is 15.9% compared to 20.2% found in the numerical results in Fedorov’s work [4].

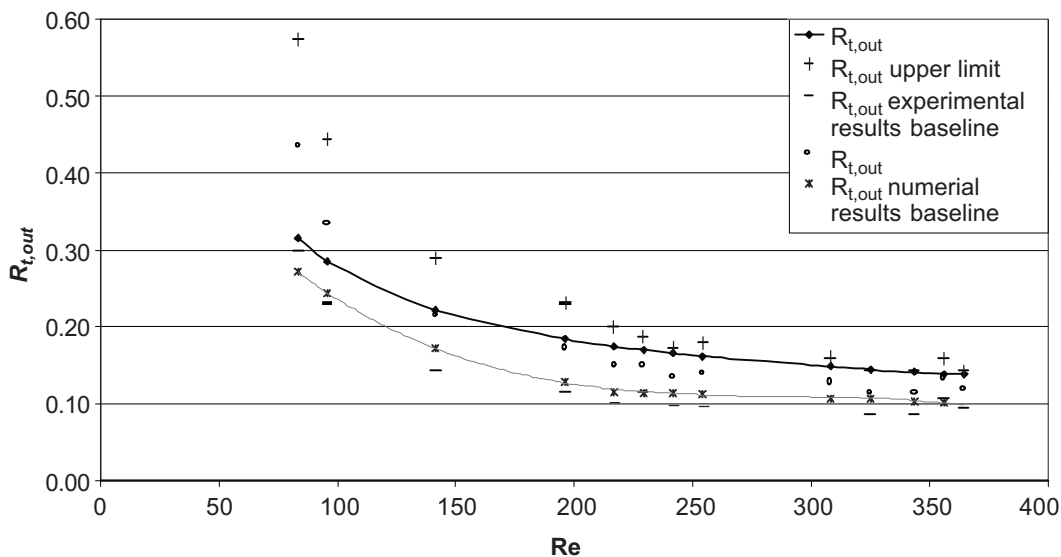


Figure 7 Model validation using thermal resistance at the outlet region

4.0 RESULTS AND DISCUSSIONS

4.1 Local Temperature Distribution

The isotherm contour plots in x - z planes are shown in Figure 8. It is found that the bottom and top wall of the heatsink demonstrate a linear temperature rise along the longitudinal direction.

The temperature change is so small that a linear temperature rise is a good approximation for the condition at the heatsink walls. However, the changes of temperature gradient in microchannel walls are distinctively large at the centre of the fluid flow at the entrance region due to the developing region of the thermal boundary layer. At the top channel wall, a reverse pattern of isotherm contour plot

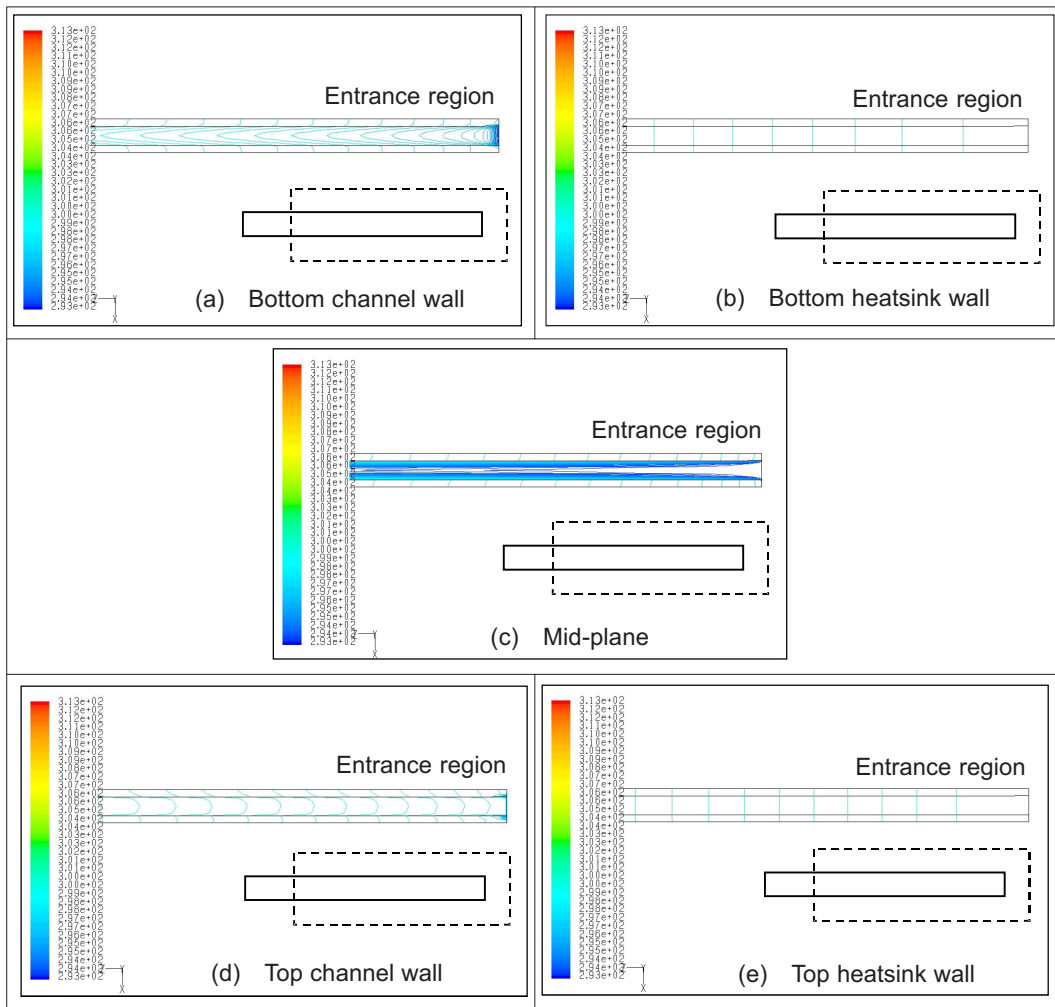


Figure 8 Isotherm contour plots of x - z planes at $Re = 140$

is noticed. This is due to the high heat flux occurring at adjacent heatsink top wall. The heat flux is efficiently spread by conduction in the upstream direction and transferred to the coolant mostly at the inlet portion of the channel. The longitudinal, upstream directed heat recirculation zones within the highly conducting walls of the channel lead to high temperature gradient at the entrance of the microchannel [4].

The isotherm contour plots at y - z planes are shown in Figure 9 for the left channel wall only due to symmetry. The temperature gradient near to the heat source (constant heat flux) is large at a given longitudinal distance- z because of the coupled effect of fluid convective cooling and heat flux from the top wall heat source. The temperature distribution within the bottom heatsink wall can be regarded as isothermal at each x - y cross section. The results discovered can direct further investigation on the design of thickness and material at the region with high temperature gradients to avoid thermal stress and hot spot effects.

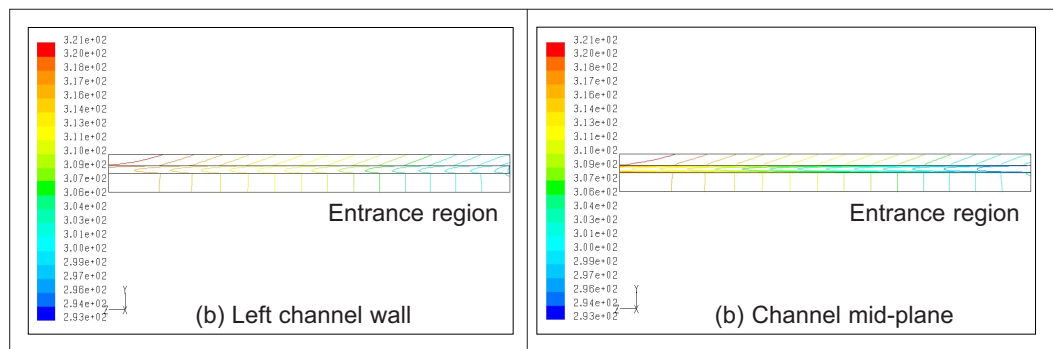


Figure 9 Isotherm contour plots of y - z planes at $Re = 140$

4.2 Local Heat Transfer Coefficients Distribution

From Figure 10, lower Reynolds number flow is shown to have a higher heat transfer coefficient in the inlet region. A slow flow of coolant with high viscous forces may have contributed to this large heat transfer in the beginning. However, the overall average heat transfer coefficient drops below that of the high Reynolds number flow for the remaining channel length.

4.3 Local Heat Flux Distribution

Figure 11 shows that increasing the flow Reynolds numbers increased the heat flux flow at top and bottom wall significantly. With increasing flow Reynolds numbers, side walls exhibit a slight decrease in heat flux near the inlet region, but increase near the outlet region. The complex pattern of heat flux distribution in the side walls may be due to the effects of the length of the developing region. Compared to the

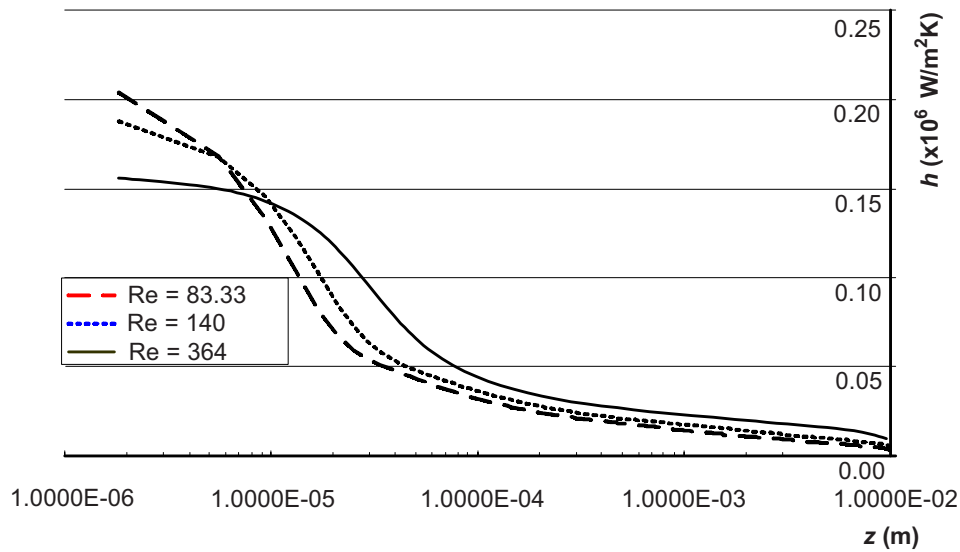


Figure 10 Heat transfer coefficient distribution along the channel length for $Re = 83.33$, 140 and 364

top and bottom walls, shorter cavity distance is found between the side walls may have caused a more dominant wall interaction effect which produces in the increase-decrease effects.

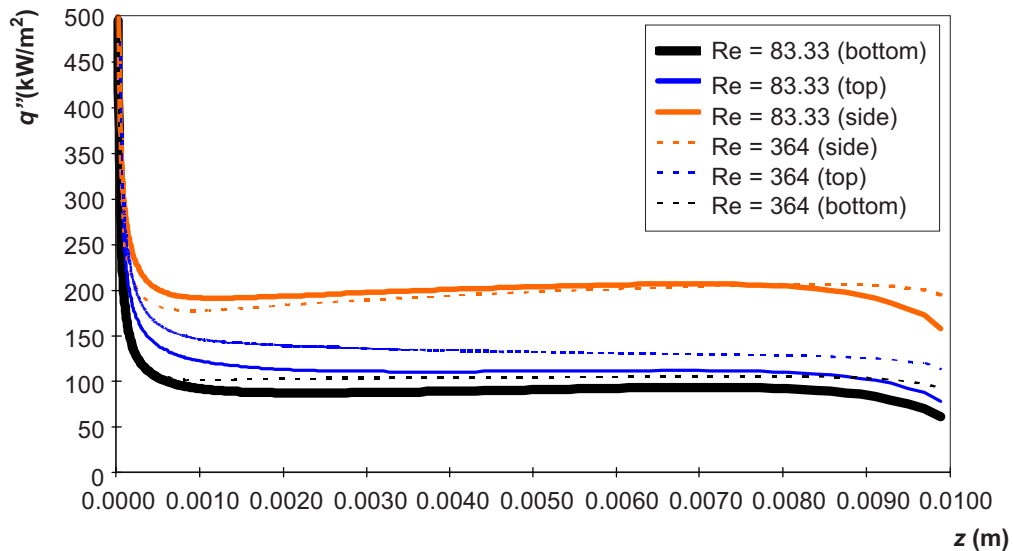


Figure 11 Average heat flux distributions at top, bottom and side walls along channel length for $Re = 83.33$, 140 and 364

4.4 Parametric Studies

Parametric study on the selected materials shows that silicon has a slightly larger average heat transfer coefficients along the channel length compared to copper and aluminum (Figure 12). However, copper was found to have the lowest thermal resistant at the outlet region (Figure 13). A lower resistance at the outlet region indicates a

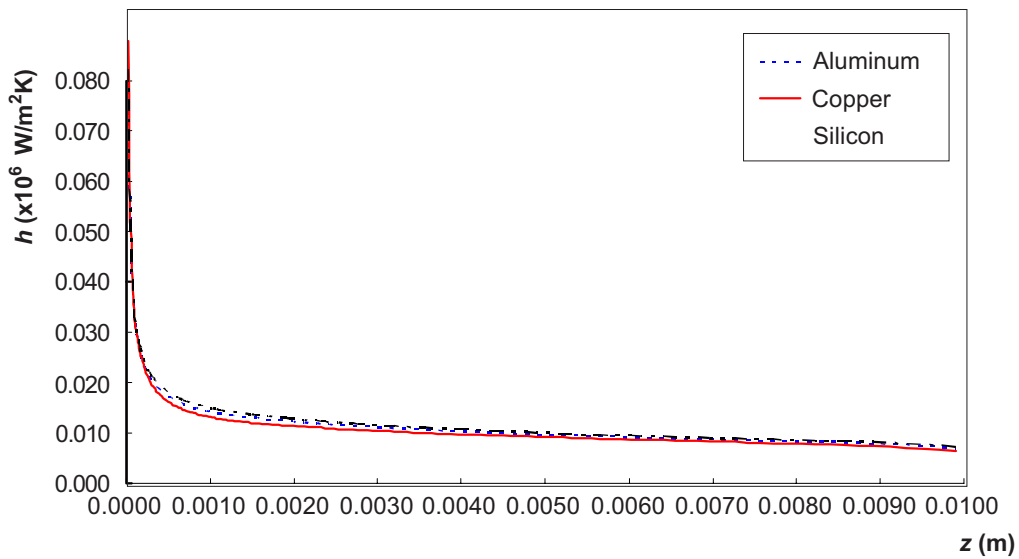


Figure 12 Average heat transfer coefficient along channel length for different materials

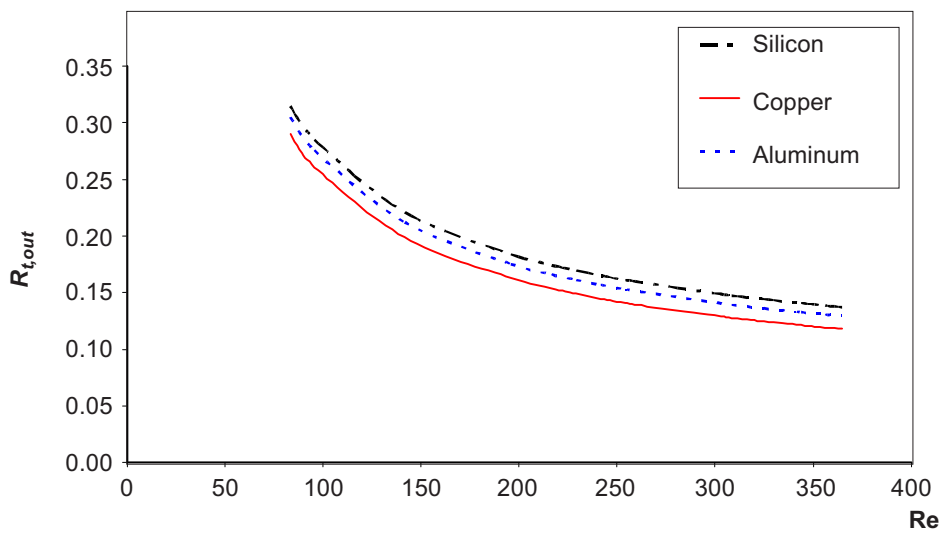


Figure 13 Thermal resistances at outlet region for different materials

better heat transfer path at that region. Silicon used in current microchannel structures may have more to do with the combination effects of its reasonable thermal resistance and other thermophysical properties relative to copper and aluminum.

Parametric study on aspect ratios shows that increase in aspect ratio leads to decrease of thermal resistance, hence increasing the thermal performance. Figure 14 shows that, with the fluid pumping power constrained, for a lower thermal resistance, a higher aspect ratio of the microchannel is required in the design. The increase of perimeter in the case of constant hydraulic diameter (denoted by curves with semi-transparent colours) increases the heat transfer rate significantly. Inversely, as the perimeter of microchannel cross section is kept constant, the thermal performance of the microchannel increase much less significantly as the aspect ratio is increased. The determinate parameter for a good thermal performance of a microchannel is its cross sectional perimeter provided that the range of hydraulics diameters for comparison purposes is not too large. It is also noted that heat transfer rate increases proportionally to cross sectional perimeter and inverse-proportionally to channel width.

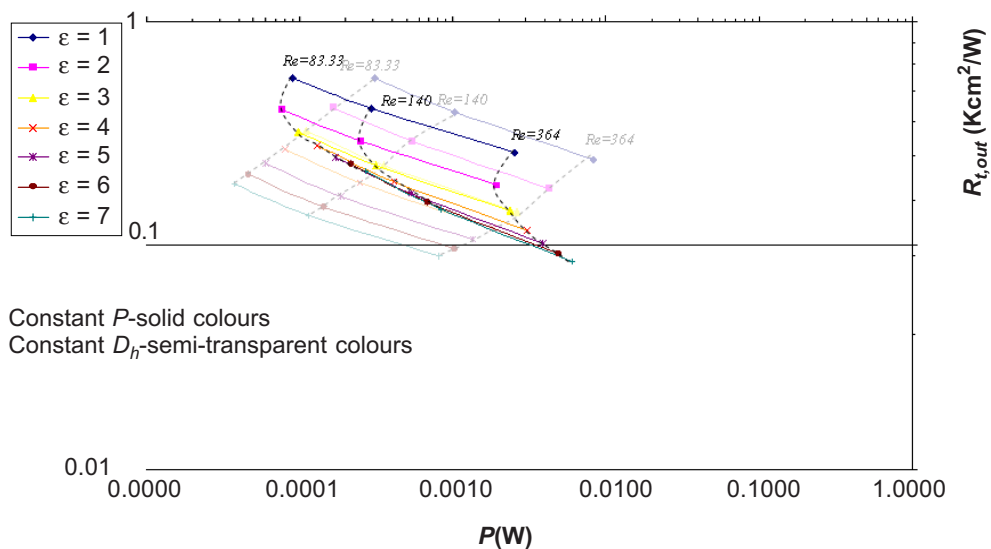


Figure 14 Comparison of aspect ratios affect on cooling capability for the cases of constant perimeter and constant hydraulics diameter

Investigation regarding the best configuration of aspect ratio in microchannel design is needed to get a higher thermal performance with less pumping power. For this investigation, a normalized value of thermal resistance and pumping power is plotted against increasing value of aspect ratios. The normalized parameter is computer as follows:

$$|R_{t,out}| = \frac{R_{t,out}}{(R_{t,out})_{max}} \tag{4}$$

$$|P_{pump}| = \frac{P_{pump}}{(P_{pump})_{max}} \tag{5}$$

The best configuration of aspect ratio is in the range of 3.7 to 4.1 (Figure 15) depending on the respective flow Reynolds number. This finding provides only a general design guideline for microchannel heatsink, limited to microchannel length of 10 mm.

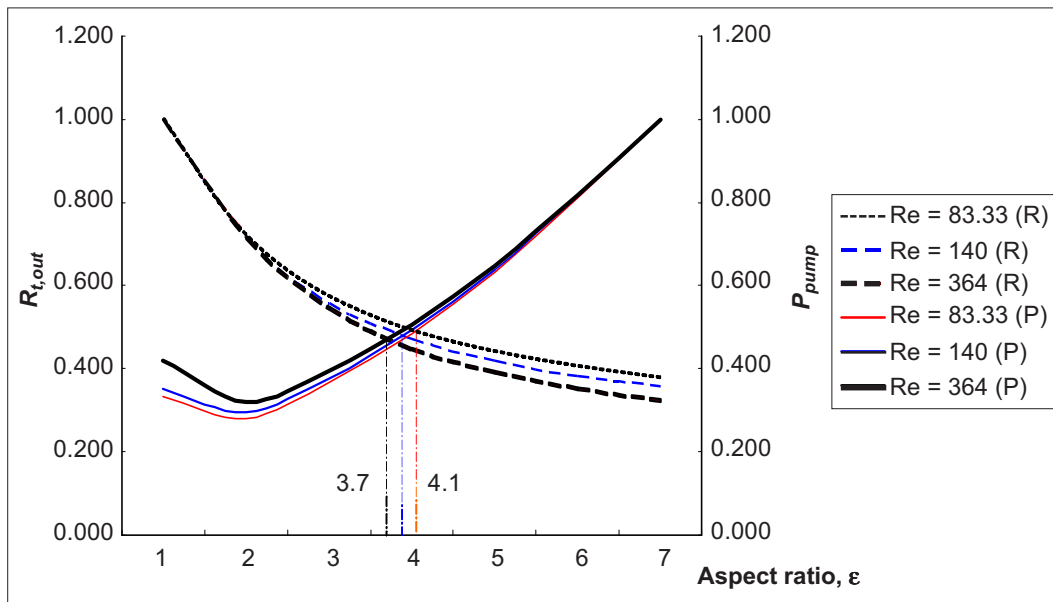


Figure 15 Optimum aspect ratio investigation using normalized thermal resistance and pumping power at Re = 83.33, 140 and 364

5.0 CONCLUSIONS

Numerical simulation of a microchannel heatsink with a flow region of 57 × 180 × 10 mm has been completed using the commercial software FLUENT. The model which takes into consideration the developing region and temperature dependent viscosity yields temperature, heat flux and thermal resistance profiles that can be used to identify regions of potential thermal stress for a better design of microchannel heatsinks. It is found that the solid domain of the channel wall near to the heat source (constant heat flux), in particular near the entrance region, has a large

temperature gradient. The temperature distribution within the bottom heatsink wall can be regarded as isothermal at each x - y cross section.

Higher Reynolds number flows generally produced a higher average heat transfer coefficient along the microchannel. Such flows also increases the heat flux at the top and bottom wall of the channel length. The side wall exhibit a decrease in heat flux except at the exit region of the channel.

Heat transfer coefficients for silicon, copper and aluminum are almost similar but silicon had a higher thermal resistance at the outlet region among the three materials tested in the simulation. This, however, is not the only factor that decides current practices in using silicon as the material in microchannel heatsinks. Silicon does have a lower density compared to copper and aluminum. Furthermore, lower thermal resistance (denoting a higher thermal performance) can be achieved with a higher aspect ratio. This is due to the reduced distance of side walls in the channel, yielding a higher velocity gradient at the wall boundaries. Findings from the present study show that heat transfer rate increases proportionally to cross sectional perimeter and inverse-proportionally to channel width. Therefore, a design of microchannel heatsink with high thermal performance can be obtained by maximizing the length of cross section perimeter and minimizing the channel width. From the investigation, the optimum aspect ratio for a 10 mm microchannel heatsink, considering the requirement of pumping power for the coolant, is around the range of 3.8 - 4.2

Future study work may include the influence of temperature-dependency of material thermophysical properties other than viscosity such as density and specific heat. The effect of pollutants and impurities in the microchannel heatsink material may also be considered. This may help us to better understand potential regions of thermal stress and hot spots in microchannel heatsink designs.

REFERENCES

- [1] Yoshi, Y. 2002. Emergency Thermal Challenges in Electronics Driven by Performance, Reliability, and Energy Efficiency. Therminic 2002. G. W. Woodruff School of Mechanical Engineering, Georgia Institute of Technology. Atlanta, USA.
- [2] Peng, X. F. and G. P. Peterson. 1996. Convective Heat Transfer and Flow Friction for Water Flow in Microchannel Structures. *Int. J. Heat Mass Transfer*. 39(12): 2599-2608.
- [3] Kawano, K, M. Y. Sekimura, K. Minakami, H. Iwasaki, and M. Ishizuka. 2001. Development of Micro Channel Heat Exchanging. *JSME International Journal*. 44(4): 592-598.
- [4] Fedorov, A. and R. Viskanta. 1999. Three-dimensional Conjugate Heat Transfer in the Microchannel Heat Sink for Electronic Packaging. *International Journal of Heat and Mass Transfer*. 43(3): 399-415.
- [5] Weilin, Q. and I. Mudawar. 2002. Analysis of Three Dimensional Heat Transfer in Microchannel Heat Sinks. *International Journal of Heat and Mass Transfer*. 45: 3973-3985.
- [6] Li, J., G. P. Peterson, and P. Cheng. 2004. Three-dimensional Analysis of Heat Transfer in a Micro-heat Sink with Single Phase Flow. *International Journal of Heat and Mass Transfer*. 47: 4215-4231.
- [7] Morini, G. L. 2004. *Single-phase Convective Heat Transfer in Microchannels: A Review of Experimental Results*. DIENCA, Università degli Studi di Bologna, Viale Risorgimento 2, Bologna, Italy.
- [8] Kakac, S., K. S. Ramesh, and W. Aung. 1987. *Handbook of Single-Phase Convective Heat Transfer*. New York: John Wiley & Son.